

Testing and improving ENSO models by process using transfer functions

Douglas G. MacMynowski¹ and Eli Tziperman²

Received 19 May 2010; revised 26 July 2010; accepted 5 August 2010; published 1 October 2010.

[1] Some key elements of ENSO are not consistently well captured in GCMs. However, modifying the wrong parameters may lead to the right result for the wrong reason. We introduce “transfer functions” to quantify the input/output relationship of individual processes from model output, to compare them to the corresponding observed processes. Two key transfer functions are calculated: first, the relationship between western Pacific Rossby waves and the reflecting Kelvin waves; second, the frequency-dependent relation between Kelvin waves traveling toward the eastern boundary and sea surface temperature response. These are estimated for TAO array data, the Cane-Zebiak model, and the GFDL CM2.1 coupled GCM. Some feedbacks are found to be biased in both models. Re-tuning parameters to fit observed transfer functions leads to a deteriorated solution, implying that compensating errors lead to the seemingly accurate simulation. This approach should be broadly useful in making climate model improvement more systematic and observation-driven. **Citation:** MacMynowski, D. G., and E. Tziperman (2010), Testing and improving ENSO models by process using transfer functions, *Geophys. Res. Lett.*, 37, L19701, doi:10.1029/2010GL044050.

1. Introduction

[2] GCMs have not been consistent in accurately capturing the dynamics of ENSO [AchutaRao and Sperber, 2006; Collins and The CMIP Modeling Groups, 2005; van Oldenborgh *et al.*, 2005] with ENSO’s average period for example ranging in state-of-the-art models from 2 to 10 years. It is often not obvious what parameters need to be changed to improve the model ENSO simulation; the ENSO cycle is the result of many individual processes and feedbacks, and a model solution may seem correct because of compensating errors in different model processes.

[3] Significant progress is being made in evaluating individual processes involved in ENSO dynamics and comparing them between models and data; see Guilyardi *et al.* [2009a] for a summary and Collins *et al.* [2010] for a focus on how these processes may change with global warming. Examples include understanding differences in the spatial characteristics of the wind stress anomalies [Capotondi *et al.*, 2006], biases in climatological currents that favor the dominance of zonal advective feedback over thermocline feedback [Dewitte *et al.*, 2007], and in error compensation due to simultaneous

underestimates of both the Bjerknes feedback and heat flux feedback [Guilyardi *et al.*, 2009b; Lloyd *et al.*, 2009].

[4] We present here an additional data analysis tool which may be used to quantify individual physical processes in terms of “transfer functions” (a term from control engineering literature) that can be estimated from both data and models. We show that this tool can lead to the identification of compensating model errors, a significant concern in climate simulation and prediction studies in general. We suggest that estimates of transfer functions of specific processes and feedbacks in ENSO models could be used as additional metrics for evaluating the “correctness” of the models. Because these metrics represent specific processes (rather than global measures such as ENSO’s amplitude or period), identifying deviations from observations or from other models may help focus on the part of the model that is in error, and may be useful in model improvement.

[5] A standard approach in the control engineering literature involves dividing a given complex system (e.g., an ENSO model) into simpler subsystems each with its input and output, and estimating the dynamics of each subsystem from time series of the input and output. Here, we apply these tools to two input/output relationships in ENSO dynamics. First, we consider the western boundary reflection coefficient (denoted T_{RK}) that relates an output Kelvin wave to an input Rossby wave; one reason for considering this process is to validate the approach taken here against prior estimates [e.g., Spall and Pedlosky, 2005; Boulanger *et al.*, 2003; Zang *et al.*, 2002]. Second, we estimate the east equatorial Pacific SST response to Kelvin wave perturbations (denoted T_{KT}). Estimates of these two relationships are compared for TAO array observations, the CZ model [Zebiak and Cane, 1987], and with the GFDL CM2.1 coupled model [Wittenberg *et al.*, 2006; van Oldenborgh *et al.*, 2005] for the present-day climate.

[6] As indicated by the above references, wave dynamics isn’t necessarily the dominant ENSO mechanism, nor the largest source of model errors in current GCMs. However, our focus on these two specific equatorial wave processes allows us to compare and discuss the new tools proposed here in the context of a well studied dynamical framework. Future work could apply this tool to other processes, including convective heating and wind response to SST anomalies, the thermocline and advective feedbacks, ocean wave forcing by wind, etc.

2. Methodology: Evaluating the Transfer Functions

[7] The frequency-dependent “transfer function” [e.g., Astrom and Murray, 2008] estimates the linear causal relationship between any pair of variables, clearly a useful

¹Control and Dynamical Systems, California Institute of Technology, Pasadena, California, USA.

²Department of Earth and Planetary Sciences, Harvard University, Cambridge, Massachusetts, USA.

tool given that key parts of ENSO's dynamics are linear to a good approximation. Thus, the relationship between Rossby (R_w) and Kelvin (K_w) wave amplitudes in the western Pacific can be written as $K_w = T_{RK}R_w$, with T_{RK} referred to here as the "reflection coefficient", though other processes may also be involved. It is convenient to first derive the (complex) transfer function directly from an example of a differential equation describing the dynamics, although as we will see below the knowledge of the governing equation is not required. For example, consider the following heuristic equation for the Niño-3 temperature T as a function of the east Pacific Kelvin wave amplitude K_e [e.g., Jin, 1997]:

$$\dot{T} = \mu K_e - \epsilon T \quad (1)$$

where μ represents the effects of the Kelvin wave on the SST via both the thermocline feedback [Dijkstra, 2000] and advective feedback [Dewitte et al., 2007] and ϵ represents dissipation processes. By taking the Fourier transform with a frequency f , we have

$$2\pi i f \hat{T}(f) = \mu \hat{K}_e(f) - \epsilon \hat{T}(f). \quad (2)$$

The transfer function is now defined by

$$T_{KT}(s) \equiv \frac{\hat{T}(s)}{\hat{K}_e(s)} = \frac{\hat{T}(s)\hat{K}_e^*(s)}{\hat{K}_e(s)\hat{K}_e^*(s)} = \mu \frac{1}{s + \epsilon}, \quad (3)$$

where $s = 2\pi i f$ and $\hat{T}(s)\hat{K}_e^*(s)$ is the cross correlation between the temperature and Kelvin wave amplitude. As this demonstrates, the transfer function depends on frequency according to the differential operator in the relation between the input and output.

[8] However, a key advantage of the approach considered here is that the equation describing the relation between the input and output does not need to be known a priori, and indeed can be extracted from time series of the two. Given input and output time series $x(t)$ and $y(t)$ and their Fourier transforms $\hat{x}(f)$ and $\hat{y}(f)$, the transfer function between them may be obtained as the ratio of the cross-correlation to the auto-correlation in frequency space, as motivated by (3) [e.g., Swanson, 2000, section 6.2]

$$T_{xy}(f) = \frac{\langle \hat{x}(f)\hat{y}^*(f) \rangle}{\langle \hat{x}(f)\hat{x}^*(f) \rangle} = \frac{S_{xy}(f)}{S_{xx}(f)}, \quad (4)$$

where $S_{xy}(f)$ is calculated by dividing the time series into n segments and averaging the respective Fourier transforms. This averaging eliminates contributions to the Niño-3 that are not related to the approaching Kelvin wave,

$$S_{xy}(f) = \frac{1}{n} \sum_{k=1}^n \hat{x}_k(f)\hat{y}_k^*(f). \quad (5)$$

See Text S1 of the auxiliary material for further technical details regarding the calculation of the transfer function, and of error estimates from the coherence [see also Swanson, 2000, equation (6.2.21)].¹ We explain there that care must be taken when interpreting the results if other processes result in a correlation between x and y , which may occur for two reasons. First, a feedback, where the output y influences

the input x in addition to x influencing y (e.g., a Kelvin wave influences eastern Pacific SST, which influences winds, which creates a Rossby wave). Second, due to correlated excitation of both the input and output variables by a third factor (e.g., western Pacific wind anomalies that simultaneously excite both Kelvin and Rossby waves).

[9] We project ocean data onto Kelvin and Rossby waves following the approach of Boulanger and Menkes [1995]; Boulanger et al. [2003] (hereafter BM95, BCM03 respectively), including their normalization, and using the 20° isotherm to estimate thermocline depth. T_{KT} is estimated as the transfer function between the Kelvin wave anomaly time series in the east Pacific at 240° (K_e) and the Niño-3 index. The resulting transfer function is not strongly dependent on the longitude used to define K_e . The transfer function T_{RK} is estimated using the Rossby and Kelvin wave amplitudes in the west Pacific at 156°, sufficiently removed from land masses close to the equator. The estimates are based on weekly averaged TAO data from 1994–2009, 22 years of weekly averaged GFDL model output, and 75 years of CZ output, all with the seasonal cycle removed. The GFDL model captures the general features of ENSO reasonably well but with too high an amplitude and possibly too short a period [Wittenberg et al., 2006]. Note that because the time scale of the two processes estimated here is short (weeks to a few months), 22 years of model output are sufficient to constrain these two transfer functions. Calculating ENSO statistics requires a longer record [Wittenberg, 2009].

3. Results: TAO Array, GFDL, and CZ Models

[10] The magnitude of the complex transfer functions representing the western boundary reflection coefficient, $|T_{RK}|$, and the response of the Niño-3 index to the Kelvin wave, $|T_{KT}|$, are shown in Figure 1 for the TAO data, GFDL model and the CZ model. Plotted error bars are 95% confidence interval (± 2 standard deviations). The best least-squares fit to a constant for $|T_{RK}|$ and μ and ϵ in equation (2) are also indicated. The results are also summarized in Table 1.

[11] Consider first the western boundary reflection, T_{RK} . In both the TAO data and the GFDL model, the transfer function estimates at frequencies above 1/(6 months) are influenced by wind disturbances that excite correlated Kelvin and Rossby waves in the western Pacific which influence the estimated transfer function but are unrelated to the reflection process. This is verified from the near-180° phase of the transfer function estimate at high frequencies (see Figure S1 and discussion in auxiliary material), and demonstrates the advantage of calculating a frequency-dependent reflection coefficient using the transfer function approach, as opposed to estimating a constant reflection coefficient directly from the two time series. At lower frequencies, the reflection coefficient is roughly independent of frequency given the error bars. Using the normalization of BCM03, the maximum possible reflection coefficient from an ideal boundary is 0.41. BCM03's estimate is 0.33–0.37, and our estimate of 0.35 from TAO data agrees well. The GFDL model ($T_{RK} = 0.28$) slightly under-estimates this transfer function. The CZ model explicitly prescribes a perfect reflection, and the estimated value is indeed close to $T_{RK} = 0.38$.

¹Auxiliary materials are available in the HTML. doi:10.1029/2010GL044050.

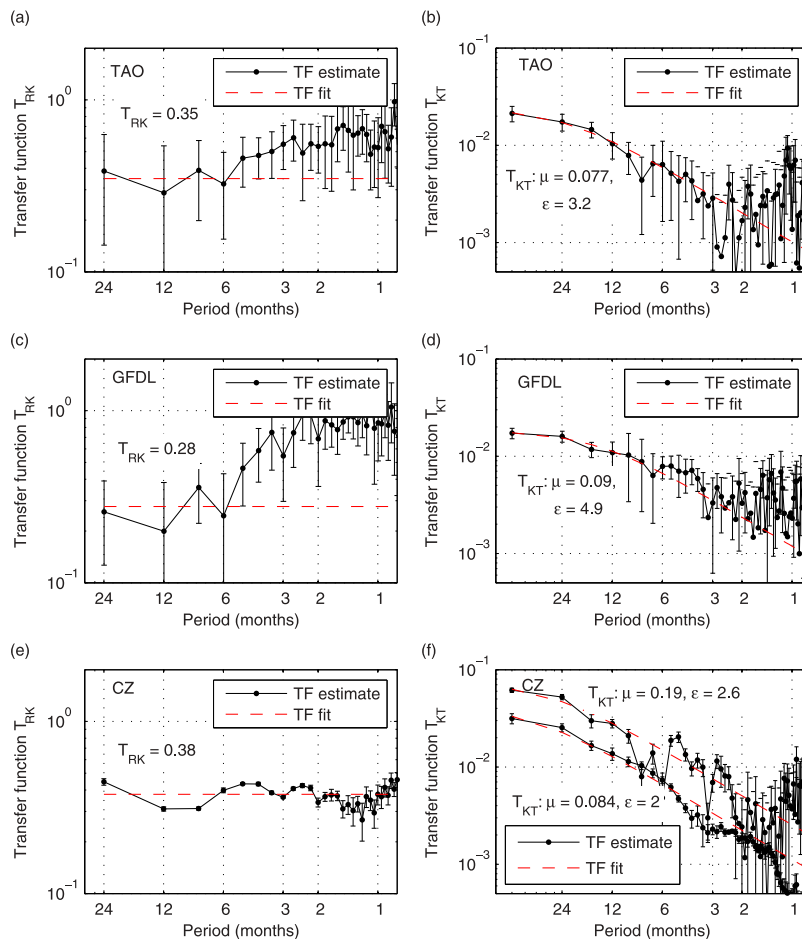


Figure 1. Transfer function magnitudes evaluated from (a and b) TAO data, (c and d) GFDL model, and (e and f) CZ model. (left) T_{RK} from western Pacific Rossby wave to western Pacific Kelvin (reflection coefficient). (right) T_{KT} from eastern Pacific Kelvin wave to Niño-3 index. The 95% confidence error bars are plotted (auxiliary material), and the red dash lines show the optimal fit to the low frequency (slower than 6 months) behavior. The CZ plot for T_{KT} includes an additional experiment (dashed), see text.

[12] The analysis of the transfer function T_{KT} from the eastern Pacific Kelvin wave anomalies to NINO3 (Figure 1, right) leads to more dramatic insights. This transfer function is found to be frequency dependent and consistent with the solution (3); this validates that the heuristic equation (1) is a reasonable description of the dynamics. The transfer function estimates allow us to identify both the strength of the feedback μ in (3) from the magnitude at mid-frequencies, and the dissipation ϵ from the frequency at which the transfer function transitions from a constant value at low frequencies to having a slope of μ/s .

[13] Based on this analysis, the GFDL model over-predicts the combined thermocline and advective feedback strength μ by $\sim 20\%$ [see also Dewitte *et al.*, 2007]. This by itself would have caused an increased coupled ocean-atmosphere instability strength, and therefore a shift in ENSO's period and amplitude. The GFDL model also shows a higher dissipation ϵ than estimated from the observations, possibly balancing the tendency toward stronger instability. This is an example of compensating errors which can be identified using transfer functions.

[14] The CZ model in its standard parameter regime over-predicts the transfer function T_{KT} even more significantly (Table 1 and Figure 1). In this case we can demonstrate the

use of these tools for tuning models in a more observationally and physically-motivated way (the comparable tuning of a GCM is, of course, less straightforward). The Kelvin wave arriving to the eastern Pacific causes an SST response there due to both perturbed upwelling and perturbed zonal advection. We find that with the standard CZ parameters, these two processes provide roughly comparable contributions to T_{KT} . Reducing both SST advection (by multiplying uT_x by a factor of one half) and the coefficient of upwelling entrainment (γ in Zebiak and Cane [1987, equation A12]) from 0.75 to 0.5, gives the additional curve in Figure 1f which is now more consistent with the TAO observations (Figure 1b). However, with these changes the CZ model is now stable, and any initial perturbations simply decay to a steady state, while in its standard parameter

Table 1. Transfer Function Results for the TAO Array Data, the GFDL Model, and the Standard Parameter Regime of the CZ Model

	$ T_{RK} $	$T_{KT}: \mu$	$T_{KT}: \epsilon^{-1}(\text{months})$
TAO	0.35	0.08	4
GFDL	0.28	0.09	2.5
CZ	0.38	0.19	4.5

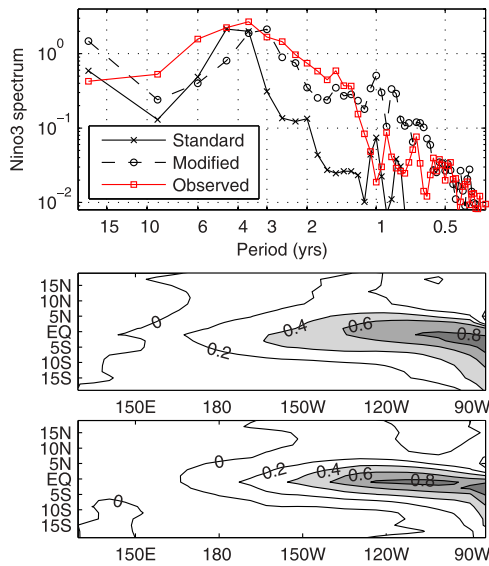


Figure 2. (top) Spectrum of Niño-3 index from the CZ model for its standard parameter regime ('x') and from a run in which the response of SST to a Kelvin wave is adjusted to be consistent with TAO observations with added stochastic forcing (dashed, 'o'). Also shown is the spectrum of the observed (1956–2009) Niño-3 index (red squares). (middle and bottom) The first EOF of the original and of the modified CZ model with the corrected SST to Kelvin wave response function.

regime the model is self-sustained. Thus, correcting the Kelvin wave influence on SST response so that it is more consistent with the observed response deteriorates the model performance significantly. This indicates that the errors in this process must have been compensated by errors in other model processes to produce the relatively realistically-looking ENSO cycle of the standard CZ model.

[15] We next added external stochastic wind perturbations to yield non-zero variability, which gives the correct value for T_{KT} . The spectrum of the model NINO3 is now flatter, and in this respect closer to the observed (Figure 2, top). The first EOF of the original and modified CZ models are shown in Figure 2 (middle and bottom) and is not any closer to observations. We cannot conclude that the missing physics is the stochastic forcing we added, and additional model transfer functions would need to be calculated in order to identify additional needed model corrections.

4. Conclusions

[16] This paper focused on two main objectives. First, by analyzing both model output and TAO array observations, we demonstrated explicitly that two ENSO models, an intermediate-complexity one and a fully coupled ocean-atmosphere general circulation model, both have compensating errors in their simulation of ENSO. Second, we introduced the calculation of “transfer functions” from time series of both observations and model output, to directly estimate specific dynamic processes from data and models. In a GCM, each process may result from a combination of parameterizations that are tuned to satisfy a difficult compromise between different aspects of the global climate. Tuning based only on some output metric, such as ENSO’s

period or amplitude or spatial characteristics, may lead to tuning of the wrong parameters and therefore to compensating errors. Our approach provides information about specific physical processes, which may make it easier to tune specific components within the model in an observationally motivated manner.

[17] The transfer functions showed that both models have significant biases in the east Pacific SST response to arriving Kelvin waves. Specifically, the GCM showed too strong an excitation of SST by the Kelvin waves, possibly partially compensated by having a too large dissipation of east Pacific SST. In the CZ model, we were able to modify some model parameters to make this process more compatible with the observed one, but this resulted in a severe deterioration of the ENSO simulation. This is direct evidence of the existence of compensating errors, as well as an example of how these tools may be used to more consistently tune and improve climate models in general and ENSO models in particular.

[18] **Acknowledgments.** We are grateful to Gabriel Vecchi for providing the GFDL model output. The ocean data were made available by the TAO Project Office of NOAA/PMEL. E.T. is funded by the NSF climate dynamics program, grant ATM-0754332 and by the NASA ECCO-II project and thanks the Weizmann institute for its hospitality during parts of this work.

References

- AchutaRao, K., and K. R. Sperber (2006), ENSO simulation in coupled ocean-atmosphere models: Are the current models better?, *Clim. Dyn.*, **27**, 1–15.
- Astrom, K. J., and R. M. Murray (2008), *Feedback Systems: An Introduction for Scientists and Engineers*, Princeton Univ. Press, Princeton, N. J.
- Boulanger, J.-P., and C. Menkes (1995), Propagation and reflection of long equatorial waves in the Pacific Ocean during the 1992–1993 El Niño, *J. Geophys. Res.*, **100**(C12), 25,041–25,059.
- Boulanger, J.-P., S. Cravatte, and C. Menkes (2003), Reflected and locally wind-forced interannual equatorial Kelvin waves in the western Pacific Ocean, *J. Geophys. Res.*, **108**(C10), 3311, doi:10.1029/2002JC001760.
- Capotondi, A., A. Wittenberg, and S. Masina (2006), Spatial and temporal structure of tropical Pacific interannual variability in 20th century coupled simulations, *Ocean Modell.*, **15**, 274–298.
- Collins, M., and The CMIP Modeling Groups (2005), El Niño- or La Niña-like climate change?, *Clim. Dyn.*, **24**, 89–104.
- Collins, M., et al. (2010), The impact of global warming on the tropical Pacific Ocean and El Niño, *Nat. Geosci.*, **3**, 391–397, doi:10.1038/NCEO868.
- Dewitte, B., C. Cibot, C. Périgaud, S.-I. An, and L. Terray (2007), Interaction between near-annual and ENSO modes in a CGCM simulation: role of equatorial background mean state, *J. Clim.*, **20**, 1035–1052.
- Dijkstra, H. A. (2000), *Nonlinear Physical Oceanography*, Kluwer Acad., Dordrecht, Netherlands.
- Guilyardi, E., A. Wittenberg, A. Fedorov, M. Collins, C. Wang, A. Capotondi, G. J. van Oldenborgh, and T. Stockdale (2009a), Understanding El Niño in ocean-atmosphere general circulation models, *Bull. Am. Meteorol. Soc.*, **90**, 325–340.
- Guilyardi, E., P. Braconnot, T. Li, F.-F. Jin, P. Kim, M. Kolasinski, and I. Musat (2009b), Mechanisms for ENSO suppression in a coupled GCM with a modified atmospheric convection scheme, *J. Clim.*, **22**, 5698–5718.
- Jin, F.-F. (1997), An equatorial ocean recharge paradigm for ENSO. Part I: Conceptual model, *J. Atmos. Sci.*, **54**, 811–829.
- Lloyd, J., E. Guilyardi, H. Weller, and J. Slingo (2009), The role of atmosphere feedbacks during ENSO in the CMIP3 models, *Atmos. Sci. Lett.*, **10**, 170–176.
- Spall, M. A., and J. Pedlosky (2005), Reflection and transmission of equatorial Rossby waves, *J. Phys. Oceanogr.*, **35**, 363–373.
- Swanson, D. C. (2000), *Signal Processing for Intelligent Sensor Systems*, Marcel Dekker, New York.
- van Oldenborgh, G. J., S. Y. Philip, and M. Collins (2005), El Niño in a changing climate: A multi-model study, *Ocean Sci.*, **1**, 81–95.

- Wittenberg, A. (2009), Are historical records sufficient to constrain ENSO simulations?, *Geophys. Res. Lett.*, *36*, L12702, doi:10.1029/2009GL038710.
- Wittenberg, A. T., A. Rosati, N. C. Lau, and J. J. Ploshay (2006), GFDL's CM2 global coupled climate models. Part III: Tropical Pacific climate and ENSO, *J. Clim.*, *19*(5), 698–722.
- Zang, X., L.-L. Fu, and C. Wunsch (2002), Observed reflectivity of the western boundary of the equatorial Pacific Ocean, *J. Geophys. Res.*, *107*(C10), 3150, doi:10.1029/2000JC000719.
- Zebiak, S. E., and M. A. Cane (1987), A model El Niño-Southern Oscillation, *Mon. Weather Rev.*, *115*, 2262–2278.
-
- D. G. MacMynowski, Control and Dynamical Systems, California Institute of Technology, 1200 E. California Blvd., M/C 107-81, Pasadena, CA 91125, USA. (macmardg@cds.caltech.edu)
- E. Tziperman, Department of Earth and Planetary Sciences and School of Engineering and Applied Sciences, Harvard University, 20 Oxford St., Cambridge, MA 02138-2902, USA. (eli@eps.harvard.edu)